Regulation of telomere metabolism by the RNA processing protein Xrn1

Cesena, Daniele; Cassani, Corinne; Rizzo, Emanuela; Lisby, Michael; Bonetti, Diego; Longhese, Maria Pia

Published in:
Nucleic Acids Research

DOI:
10.1093/nar/gkx072

Publication date:
2017

Document version
Publisher's PDF, also known as Version of record

3860–3874 *Nucleic Acids Research, 2017, Vol. 45, No. 7* *Published online 4 February 2017*
doi: 10.1093/nar/gkx072

Regulation of telomere metabolism by the RNA processing protein Xrn1

Daniele Cesena[1], Corinne Cassani[1], Emanuela Rizzo[1], Michael Lisby[2], Diego Bonetti[1] and Maria Pia Longhese[1,*]

[1]Dipartimento di Biotecnologie e Bioscienze, Università di Milano-Bicocca, Milan 20126, Italy and [2]Department of Biology, University of Copenhagen, DK-2200 Copenhagen N, Denmark

Received July 4, 2016; Revised January 23, 2017; Editorial Decision January 25, 2017; Accepted January 25, 2017

ABSTRACT

Telomeric DNA consists of repetitive G-rich sequences that terminate with a 3′-ended single stranded overhang (G-tail), which is important for telomere extension by telomerase. Several proteins, including the CST complex, are necessary to maintain telomere structure and length in both yeast and mammals. Emerging evidence indicates that RNA processing factors play critical, yet poorly understood, roles in telomere metabolism. Here, we show that the lack of the RNA processing proteins Xrn1 or Rrp6 partially bypasses the requirement for the CST component Cdc13 in telomere protection by attenuating the activation of the DNA damage checkpoint. Xrn1 is necessary for checkpoint activation upon telomere uncapping because it promotes the generation of single-stranded DNA. Moreover, Xrn1 maintains telomere length by promoting the association of Cdc13 to telomeres independently of ssDNA generation and exerts this function by downregulating the transcript encoding the telomerase inhibitor Rif1. These findings reveal novel roles for RNA processing proteins in the regulation of telomere metabolism with implications for genome stability in eukaryotes.

INTRODUCTION

Nucleoprotein complexes called telomeres are present at the ends of linear eukaryotic chromosomes, where they ensure replication of the chromosome ends and prevent their recognition as DNA double-strand breaks (DSBs) (1,2). Telomeric DNA in most eukaryotes consists of tandem arrays of short repeated sequences which are guanine-rich in the strand running 5′-3′ from the centromere toward the chromosome end. The G-rich strand at both ends of a chromosome extends over the C-strand to form a 3′-ended single-stranded G-rich overhang (G-tail) (3,4). This G-tail is important for telomere replication, because it provides a substrate for the telomerase enzyme. Telomerase is a ribonucleoprotein complex that uses its RNA component as a template to elongate the telomere by addition of G-rich telomeric repeats to the G-tail (1,5). The telomerase-extended single-stranded DNA (ssDNA) must then be copied by the conventional replication machinery to reconstitute the double-stranded telomeric DNA.

In *Saccharomyces cerevisiae*, single-stranded G-rich tails of 5–10 nt in length are present at telomeres throughout most of the cell cycle except in late S phase, when longer overhangs are detected (4,6,7). Removal of the last RNA primers that are generated by lagging-strand synthesis appears to match the observed overhang length (8). By contrast, the telomeric C-strands generated by leading-strand synthesis are resected by about 30–40 nt before being filled in again to leave DNA ends with a 3′ overhang of about 10 nt (8,9). This resection depends on the MRX (Mre11-Rad50-Xrs2) complex, on the exonuclease Exo1 and on the Sgs1-Dna2 helicase-nuclease complex (10–12).

G-tails at both leading- and lagging-strand telomeres are covered by the CST (Cdc13-Stn1-Ten1) complex, which is an RPA-like complex that binds with high affinity and sequence specificity to the telomeric ssDNA overhangs (13). The CST complex drives the localization of telomerase to telomeres through a direct interaction between Cdc13 and the telomerase subunit Est1 (14–17). MRX, in turn, ensures robust association of telomerase with telomeres by promoting the binding of the checkpoint kinase Tel1 via a specific interaction with the MRX subunit Xrs2 (18–22). It remains unclear whether Tel1 facilitates telomerase association directly by phosphorylating specific targets that promote telomerase recruitment, and/or indirectly by stimulating resection of the C-strand, thus generating a ssDNA substrate for telomerase action (23–25). Interestingly, Mre11 inactivation strongly reduces the binding to telomeres of the telomerase subunits Est1 and Est2, while it has a moderate effect on Cdc13 binding (26). Further work has shown that the absence of Mre11 reduces Cdc13 binding only to the leading-strand telomere, while Cdc13 ability to bind to the lagging-strand telomere is not affected (9). This observation

*To whom correspondence should be addressed. Tel: +39 02 64 483 425; Fax: +39 02 64 483 565; Email: mariapia.longhese@unimib.it

is consistent with the finding that Mre11 binds only to leading telomeres to generate the single-stranded overhangs (9).

In addition to drive telomerase localization to telomeres, the CST complex also genetically and physically interacts with the DNA polymerase α/primase complex and promotes lagging strand synthesis during telomere replication (27,28). Furthermore, it prevents inappropriate generation of ssDNA at telomeric ends. Cdc13 inactivation through either the *cdc13-1* temperature sensitive allele or the *cdc13-td* conditional degron allele results in both degradation of the 5′-terminated DNA strand and checkpoint-mediated cell cycle arrest (29–31). Similarly, temperature sensitive alleles of either the *STN1* or *TEN1* gene cause telomere degradation and checkpoint-dependent cell cycle arrest at the non-permissive temperature (32–35). DNA degradation in the *cdc13-1* mutant depends mainly on the 5′-3′ nuclease Exo1 (36,37), suggesting that CST protects telomeric DNA from Exo1 activity.

There is emerging evidence that telomere metabolism is influenced by RNA processing pathways. In eukaryotes, RNA processing relies on two highly conserved pathways involving both 5′-3′ and 3′-5′ exoribonuclease activities (38). In particular, 5′-3′ degradation is performed by the Xrn protein family, which comprises the cytoplasmic Xrn1 enzyme and the nuclear Rat1 enzyme (also known as Xrn2) (39). The 3′-5′ RNA processing activity is due to the exoribonuclease Rrp6 that belongs to the nuclear exosome (40). In addition, RNA molecules are subjected to a quality control system, which is called nonsense-mediated mRNA decay (NMD) and degrades non-functional RNAs that might otherwise give rise to defective protein products (38).

RNA processing proteins have been recently implicated in telomere metabolism in both yeast and mammals, although the related mechanisms are poorly understood. In particular, Xrn1 has been identified in genome-wide screenings for *S. cerevisiae* mutants with altered telomere length (41,42). Moreover, proteins belonging to the mammalian NMD pathway have been found to bind telomeres and to control telomere length (43,44). Similarly, the lack of the *S. cerevisiae* NMD proteins was shown to cause telomere shortening by increasing the amount of Stn1 and Ten1, which in turn inhibit telomerase activity by interfering with Est1–Cdc13 interaction (45–48). Furthermore, both Xrn1 and the nuclear exosome control degradation of the RNA component of human telomerase (49). Finally, Rat1 and the NMD pathway control the level of a new class of non-coding RNAs called TERRA (telomeric repeat-containing RNA), which are transcribed from the subtelomeric sequences and likely regulate telomere length (50–52).

Here we show that the lack of the *S. cerevisiae* RNA processing factors Xrn1 or Rrp6 suppresses the temperature sensitivity of *cdc13-1* mutant cells by attenuating the activation of the DNA damage checkpoint response. In particular, Xrn1 is required to activate the checkpoint upon telomere uncapping because it promotes the generation of ssDNA. Furthermore, Xrn1 maintains telomere length independently of ssDNA generation by promoting Cdc13 association to telomeres through downregulation of the transcript encoding the telomerase inhibitor Rif1.

MATERIALS AND METHODS

Strains and plasmids

Strain genotypes are listed in Supplementary Table S1. Strains used for monitoring telomere addition were derivatives of strain UCC5913, kindly provided by D. Gottschling (Fred Hutchinson Cancer Research Center, Seattle, USA). Strains ML968-1D and ML968-3B are derivatives of ML8-9A, a *RAD5 ADE2* derivative of W303 (*MAT***a** *LYS2 ade2-1 can1-100 ura3-1 his3-11,15 leu2-3, 112 trp1-1 rad5-535*). A plasmid carrying the *GAL1-RNH1* allele and the control vector plasmid *pGAL1* were kindly provided by A. Aguilera (University of Seville, Sevilla, Spain). Plasmids pAM140/pAJ228 (*CEN LEU2 rat1-ΔNLS*), pAM144 (*CEN LEU2 xrn1-E176G*) and pAM145/pAJ37 (*CEN LEU2 XRN1*) were kindly provided by A.W. Johnson (University of Texas, Austin, USA). Plasmid pGFPRRP6H1 (*CEN URA3* pGFP-*rrp6-D238A*) was kindly provided by J.S. Butler (University of Rochester Medical Center, Rochester, USA). Plasmid pTRP61 (2μ *TRP1 GAL1-TLC1*) was kindly provided by R. Wellinger (Université de Sherbrooke, Québec, Canada). Plasmid pVL1091 (*CEN LEU2 CDC13-EST1*) was kindly provided by V. Lundblad (Salk Institute, La Jolla, USA). All gene disruptions were carried out by polymerase chain reaction (PCR)-based methods. The accuracy of all gene replacements and integrations was verified by Southern blot analysis or PCR. Cells were grown in YEP medium (1% yeast extract, 2% bactopeptone, 50 mg/l adenine) supplemented with 2% glucose (YEPD) or 2% raffinose (YEPR) or 2% raffinose and 2% galactose (YEPRG).

Southern blot analysis of telomere length

The length of HO (Homothallic)-induced telomeres was determined as previously described (53). Briefly, yeast DNA was digested with SpeI and the resulting DNA fragments were separated by 0.8% agarose gel electrophoresis and hybridized with a ^{32}P-labeled probe corresponding to a 500 bp *ADE2* fragment. To determine the length of native telomeres, XhoI-digested yeast DNA was subjected to 0.8% agarose gel electrophoresis and hybridized with a ^{32}P-labeled poly(GT) probe. Standard hybridization conditions were used.

ChIP and qPCR

ChIP analysis was performed as previously described (54). Quantification of immunoprecipitated DNA was achieved by quantitative real-time PCR (qPCR) on a Bio-Rad MiniOpticon apparatus. Triplicate samples in 20 μl reaction mixture containing 10 ng of template DNA, 300 nM for each primer, 2× SsoFast™ EvaGreen® supermix (Bio-rad #1725201) were run in white 48-well PCR plates Multiplate™ (Bio-Rad #MLL4851). The qPCR program was as follows: step 1, 98°C for 2 min; step 2, 98°C for 5 s; step 3, 60°C for 10 s; step 4, return to step 2 and repeat 30 times. At the end of the cycling program, a melting program (from 65 to 95°C with a 0.5°C increment every 5 s) was run to test the specificity of each qPCR. qPCR at the HO-induced telomere was carried out by using primer pairs located at 640 bp

centromere-proximal to the HO cutting site at chromosome VII and at the non-telomeric *ARO1* fragment of chromosome IV (CON). qPCR at native telomeres was carried out by using primer pairs located at 70 and 139 bp from the TG sequences on telomeres VI-R (right) and XV-L (left), respectively. Data are expressed as fold enrichment over the amount of CON in the immunoprecipitates after normalization to input signals for each primer set.

qRT-PCR

Total RNA was extracted from cells using the Bio-Rad Aurum total RNA mini kit. First strand cDNA synthesis was performed with the Bio-Rad iScript™ cDNA Synthesis Kit. qRT-PCR was performed on a MiniOpticon Real-time PCR system (Bio-Rad) and RNA levels were quantified using the ΔΔCt method. Quantities were normalized to *ACT1* RNA levels and compared to that of wild-type cells that was set up to 1. Primer sequences are available upon request.

Fluorescence microscopy

Yeast cells were grown and processed for fluorescence microscopy as described previously (55). Fluorophores were cyan fluorescent protein (CFP, clone W7) (56) and yellow fluorescent protein (YFP, clone 10C) (57). Fluorophores were visualized on a Deltavision Elite microscope (Applied Precision, Inc) equipped with a 100× objective lens (Olympus U-PLAN S-APO, NA 1.4), a cooled Evolve 512 EM-CCD camera (Photometrics, Japan) and an Insight solid state illumination source (Applied Precision, Inc). Pictures were processed with Volocity software (PerkinElmer). Images were acquired using softWoRx (Applied Precision, Inc) software.

Other techniques

Visualization of the single-stranded overhangs at native telomeres was done as previously described (6). The same gel was denatured and hybridized with the end-labeled C-rich oligonucleotide for loading control. Protein extracts to detect Rad53 were prepared by trichloroacetic acid (TCA) precipitation. Rad53 was detected using anti-Rad53 polyclonal antibodies from Abcam. Secondary antibodies were purchased from Amersham and proteins were visualized by an enhanced chemiluminescence system according to the manufacturer.

RESULTS

The lack of Xrn1 or Rrp6 partially suppresses the temperature sensitivity of *cdc13-1* cells

Protection of telomeres from degradation depends on the CST (Cdc13-Stn1-Ten1) complex, which specifically binds to the telomeric ssDNA overhangs (13). We have previously shown that the RNA processing proteins Xrn1 and Rrp6 are required to fully activate the checkpoint kinase Mec1/ATR at intrachromosomal DSBs (58). We then asked whether Xrn1 and/or Rrp6 regulate checkpoint activation also in response to telomere uncapping. To this end, we analyzed the effect of deleting either the *XRN1* or the *RRP6* gene in *cdc13-1* cells, which show temperature-dependent loss of telomere capping, ssDNA production, checkpoint activation and cell death (29,30). As expected, *cdc13-1* cells were viable at permissive temperature (25°C), but died at restrictive temperature (26–30°C) (Figure 1A). Deletion of either *XRN1* or *RRP6* partially suppressed the temperature sensitivity of *cdc13-1* cells, as it allowed *cdc13-1* cells to form colonies at 26–28°C (Figure 1A). Xrn1 and Rrp6 appear to impair cell viability of *cdc13-1* cells by acting in two different pathways, as *xrn1Δ rrp6Δ cdc13-1* triple mutant cells formed colonies at 30°C more efficiently than both *xrn1Δ cdc13-1* and *xrn1Δ cdc13-1* double mutant cells (Figure 1B).

Xrn1 and Rrp6 control RNA degradation by acting as 5′-3′ and 3′-5′ exoribonucleases, respectively (38). The *xrn1-E176G* and *rrp6-D238A* alleles, encoding nuclease-defective Xrn1 or Rrp6 variants (59,60), suppressed the temperature sensitivity of *cdc13-1* cells to an extent similar to that of *xrn1Δ* and *rrp6Δ*, respectively (Figure 1C). Therefore, Xrn1 and Rrp6 appear to impair viability in the presence of uncapped telomeres by acting as nucleases.

Xrn1 controls cytoplasmic RNA decay, whereas RNA processing in the nucleus depends on its nuclear paralog Rat1 (61). Targeting Rat1 to the cytoplasm by deleting its nuclear localization sequence (*rat1-ΔNLS*) restores Xrn1-like function in RNA degradation (61), prompting us to ask whether it could restore Xrn1 function in causing loss of viability of *cdc13-1* cells. Strikingly, *cdc13-1 xrn1Δ* cells expressing the *rat1-ΔNLS* allele on a centromeric plasmid formed colonies at 27°C much less efficiently than *cdc13-1 xrn1Δ* cells expressing wild type *RAT1* (Figure 1D). Thus, Xrn1 impairs viability in the presence of uncapped telomeres by controlling a cytoplasmic RNA decay pathway.

Xrn1 and Rrp6 are required to fully activate the checkpoint at uncapped telomeres

A checkpoint-dependent arrest of the metaphase to anaphase transition is observed in *cdc13-1* cells at high temperatures (29). Failure to turn on the checkpoint allows *cdc13-1* cells to form colonies at 28°C (30), indicating that checkpoint activation can partially account for the loss of viability of *cdc13-1* cells. We therefore asked whether the enhanced temperature resistance of *cdc13-1 xrn1Δ* and *cdc13-1 rrp6Δ* cells might be related to defective checkpoint activation. Cell cultures were arrested in G1 with α-factor at 23°C and then released from G1 arrest at 28°C, followed by monitoring nuclear division at different time points. As expected, *cdc13-1* cells remained arrested as large budded cells with a single nucleus throughout the experiment (Figure 2A). Conversely, although *xrn1Δ* and *rrp6Δ* single mutant cells slowed down nuclear division compared to wild type cells, *cdc13-1 xrn1Δ* and *cdc13-1 rrp6Δ* cells started to divide nuclei about 90 min after release (Figure 2A).

We then examined under the same conditions phosphorylation of the Rad53 checkpoint kinase that is necessary for checkpoint activation and can be detected as changes in Rad53 electrophoretic mobility. After release at 28°C from G1 arrest, Rad53 phosphorylation was strong in *cdc13-1* cells, as expected, whereas it was undetectable in *cdc13-1 xrn1Δ* cells and it was reduced in *cdc13-1 rrp6Δ* cells (Figure 2B). Taken together, these results indicate that Xrn1

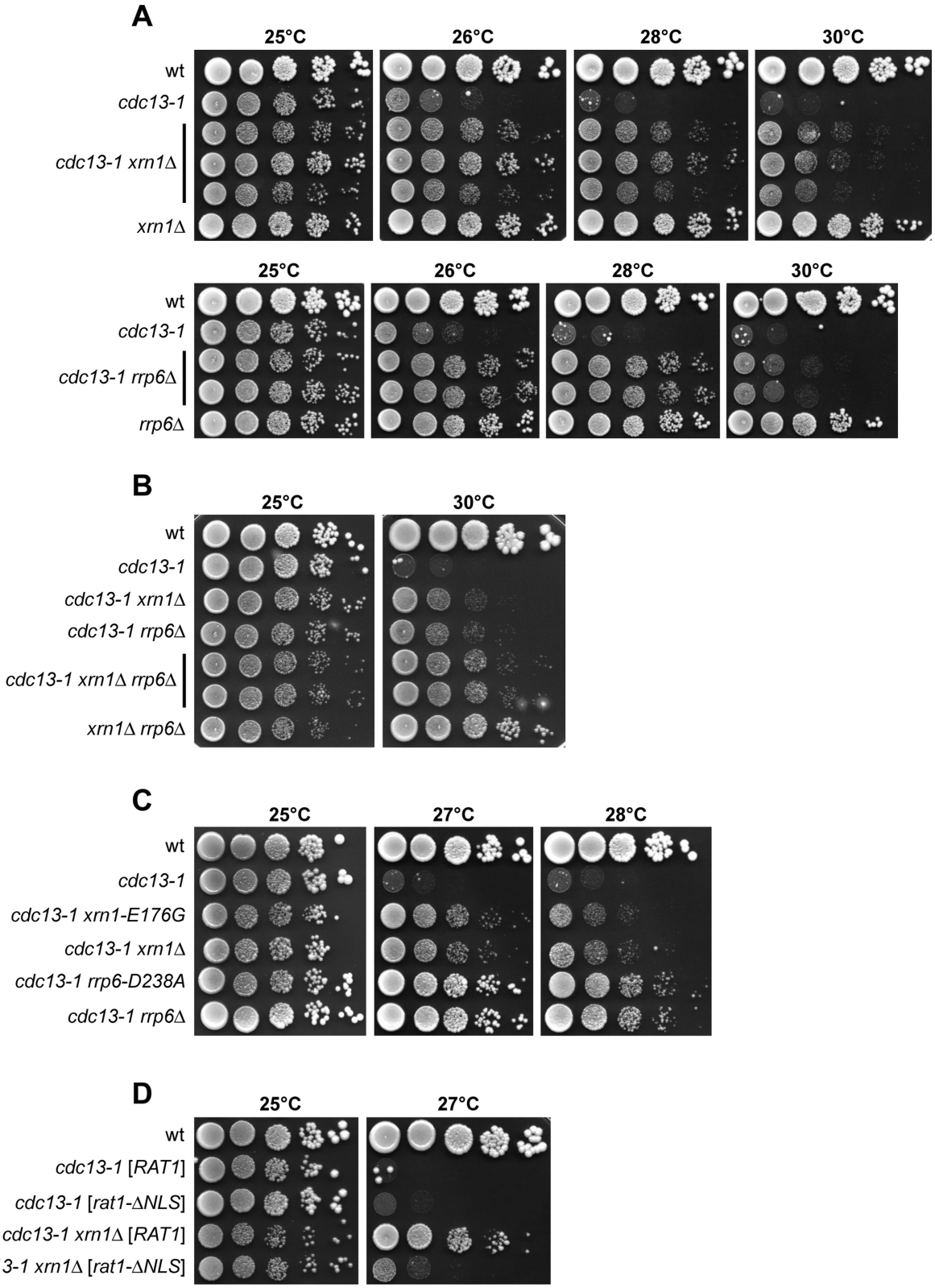

Figure 1. The lack of Xrn1 or Rrp6 partially suppresses the temperature sensitivity of *cdc13-1* cells. (**A**–**D**) Cell cultures were grown overnight at 23°C and 10-fold serial dilutions were spotted onto YEPD plates. Bars point out independent clones. Plates were incubated at the indicated temperatures before images were taken.

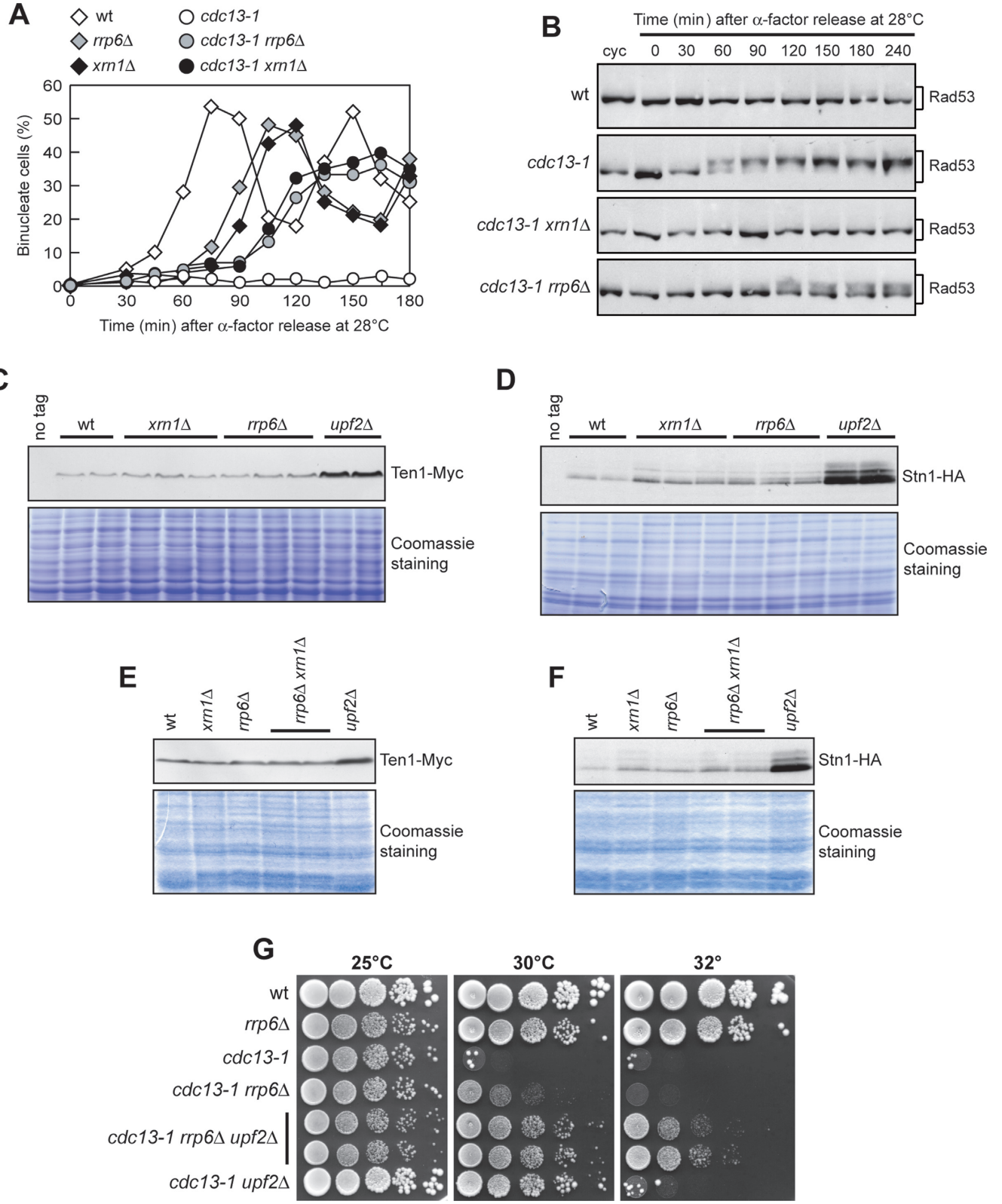

Figure 2. The lack of Xrn1 or Rrp6 reduces checkpoint activation in *cdc13-1* cells and suppresses the temperature sensitivity of *cdc13-1* cells by acting in a pathway different from NMD. (**A** and **B**) Cell cultures exponentially growing at 23°C in YEPD (cyc) were arrested in G1 with α-factor and then released into the cell cycle at 28°C (time zero). Samples were taken at the indicated times after α-factor release to determine the kinetics of nuclear division (A), and for western blot analysis of protein extracts using anti-Rad53 antibodies (B). (**C**–**F**) Protein extracts prepared from cell cultures exponentially growing at 25°C in YEPD were subjected to western blot analysis with anti-Myc (C and E) and anti-HA (D and F) antibodies. The same amount of extracts was separated by SDS-PAGE and stained with Coomassie Blue as loading control. Bars point out two or three independent cell cultures. (**G**) Cell cultures were grown overnight at 23°C and 10-fold serial dilutions were spotted onto YEPD plates. The bar points out two independent clones.

and Rrp6 are required to fully activate the checkpoint in response to telomere uncapping caused by defective Cdc13.

Xrn1 and Rrp6 regulate telomere capping through a mechanism that is distinct from that involving the NMD pathway

In both yeast and mammals, the NMD pathway is involved in quality control of gene expression by eliminating aberrant RNAs (62). Interestingly, NMD inactivation was shown to suppress the temperature sensitivity of *cdc13-1* cells by increasing the levels of the Cdc13 interacting proteins Stn1 and Ten1, which likely stabilize the CST complex at telomeres (46,47,63). These high levels of Stn1 and Ten1 are also responsible for the short telomere length phenotype of *nmdΔ* mutants, possibly because Stn1 and Ten1 inhibit telomerase activity by interfering with Est1–Cdc13 interaction (16,34,64,65).

As 77% of the transcripts that are upregulated in *nmdΔ* cells are upregulated also in *xrn1Δ* cells (66), we asked whether Xrn1 and/or Rrp6 action at telomeres might involve the same pathway that is regulated by NMD. To this purpose, we constructed fully functional Ten1-Myc and Stn1-HA alleles to analyze the levels of Ten1 and Stn1 in *xrn1Δ* and *rrp6Δ* cells. As expected, the amounts of Ten1-Myc and Stn1-HA were greatly increased in cells lacking the NMD protein Upf2 (Figure 2C and D). By contrast, the lack of Xrn1 or Rrp6 did not change the amount of Ten1-Myc (Figure 2C) and only very slightly increased the amount of Stn1-HA (Figure 2D). Furthermore, Xrn1 and Rrp6 do not compensate for the absence of each other in controlling Ten1 and Stn1 levels, as the amount of Ten1-Myc (Figure 2E) and Stn1-HA (Figure 2F) in *xrn1Δ rrp6Δ* double mutant cells was similar to that in *xrn1Δ* and *rrp6Δ* single mutant cells.

The presence of the Myc or HA tag at the C-terminus of Ten1 and Stn1, respectively, did not affect the possible regulation of the corresponding mRNAs by Xrn1 or Rrp6, as the suppression of the temperature sensitivity of *cdc13-1* cells by *XRN1* or *RRP6* deletion was similar either in the presence or in the absence of the *TEN1-MYC* or *STN1-HA* allele (Supplementary Figure S1).

We also analyzed the epistatic relationships between Xrn1/Rrp6 and NMD. The effect of deleting *UPF2* in *xrn1Δ cdc13-1* cells could not be assessed due to the poor viability of the triple mutant at 23–25°C. Nonetheless, deletion of *UPF2*, which partially suppressed the temperature sensitivity of *cdc13-1* cells, further improved the temperature resistance of *cdc13-1 rrp6Δ* double mutant cells at 32°C compared to both *cdc13-1 rrp6Δ* and *cdc13-1 upf2Δ* cells (Figure 2G). Altogether, these data suggest that Xrn1 and Rrp6 impair survival of *cdc13-1* by acting in a pathway that is different from that involving the NMD proteins.

Xrn1 is required to generate ssDNA at uncapped telomeres

It is known that cell death of *cdc13-1* cells at restrictive temperatures is due to generation of telomeric ssDNA that triggers checkpoint-mediated metaphase arrest (29,30). Hence, the improved temperature resistance of *cdc13-1 xrn1Δ* and *cdc13-1 rrp6Δ* cells might be due to a reduction of the amount of telomeric DNA that becomes single-stranded in *cdc13-1* cells at restrictive temperatures. We therefore assessed the presence of ssDNA at natural chromosome ends by analyzing genomic DNA prepared from exponentially growing cells. Non-denaturing in-gel hybridization with a C-rich radiolabeled oligonucleotide showed that the amount of telomeric ssDNA after incubation of cells at 28°C for 5 h was lower in *cdc13-1 xrn1Δ* double mutant cells than in *cdc13-1* cells (Figure 3A). By contrast, the level of single-stranded TG sequences showed a very similar increase in both *cdc13-1* and *cdc13-1 rrp6Δ* mutant cells compared to wild type cells (Figure 3A).

The function of Cdc13 in telomere protection is mediated by its direct interaction with Stn1 and Ten1. In contrast to Cdc13, Stn1 inhibits telomerase action by competing with Est1 for binding to Cdc13 (64,65). As a consequence, cells lacking the Stn1 C-terminus (*stn1-ΔC*) display long telomeres because the Stn1-ΔC variant fails to compete with Est1 for binding to Cdc13. Furthermore, these same cells accumulate telomeric ssDNA, although the amount of this ssDNA is not enough to impair cell viability (34,64,67). We therefore evaluated the specificity of the genetic interactions between Cdc13, Xrn1 and Rrp6 by analyzing the consequences of deleting *XRN1* or *RRP6* in *stn1-ΔC* cells. Like in *cdc13-1* cells, generation of telomeric ssDNA in *stn1-ΔC* cells was reduced by the lack of Xrn1, but not by *RRP6* deletion (Figure 3B). Thus, Xrn1 is required to generate ssDNA at dysfunctional telomeres, whereas Rrp6 does not, implying that the defective checkpoint response in *cdc13-1 rrp6Δ* cells cannot be ascribed to a reduced generation of telomeric ssDNA.

The data above suggest that the lack of Xrn1 might suppress the temperature sensitivity of *cdc13-1* cells by attenuating the generation of telomeric ssDNA. We then asked whether the overexpression of Exo1, which bypasses MRX requirement for intrachromosomal DSB end resection (68), decreased the maximum permissive temperature of *cdc13-1 xrn1Δ* cells. Strikingly, *cdc13-1 xrn1Δ* cells containing the *EXO1* gene on a 2μ plasmid were more temperature-sensitive than *cdc13-1 xrn1Δ* cells containing the empty vector (Figure 3C). This finding supports the hypothesis that the lack of Xrn1 can partially bypass the requirement for CST in telomere capping because it attenuates the generation of telomeric ssDNA.

Xrn1 maintains telomere length by acting as a cytoplasmic nuclease

Xrn1 has been identified in genome-wide screenings for *S. cerevisiae* mutants that are affected in telomere length (41,42). We confirmed the requirement for Xrn1 in telomere elongation by using an inducible short telomere assay that allows the generation of a single short telomere without affecting the length of the other telomeres in the same cell (10). We used a strain that carried at the *ADH4* locus on chromosome VII an internal tract of telomeric DNA sequence (81 bp TG) adjacent to an HO endonuclease recognition sequence (Figure 4A) (10,69). Upon cleavage by HO, the fragment distal to the break is lost, and, over time, the TG side of the break is elongated by the telomerase. As shown in Figure 4B, sequence addition at the HO-derived telomere was clearly detectable after galactose addition in

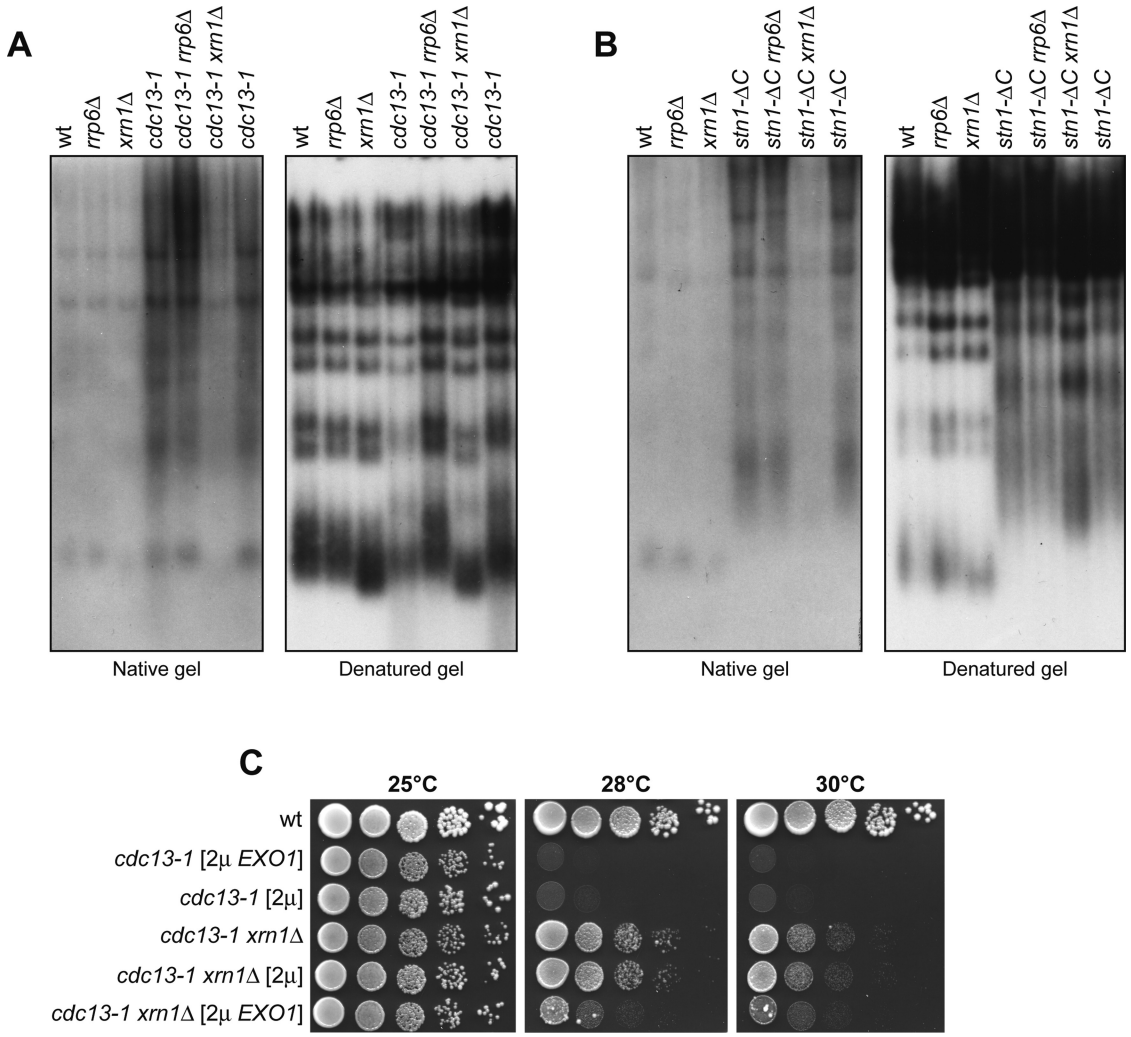

Figure 3. The lack of Xrn1 reduces ssDNA generation at uncapped telomeres. (**A** and **B**) Cell cultures exponentially growing at 23°C were shifted to 28°C for 5 h. Genomic DNA was digested with XhoI, and single-stranded G-tails were visualized by non-denaturing in-gel hybridization (native gel) using an end-labeled C-rich oligonucleotide as a probe. The gel was denatured and hybridized again with the same probe for loading control (denatured gel). (**C**) Cell cultures were grown overnight and 10-fold serial dilutions were spotted onto YEPD plates. Plates were incubated at the indicated temperatures before images were taken.

wild type cells, whereas it was strongly delayed and reduced in *xrn1Δ* cells, confirming the requirement for Xrn1 in telomere elongation.

Xrn1 controls telomere length by acting as cytoplasmic nuclease. In fact, expression of the Xrn1 nuclear paralog Rat1 lacking its nuclear localization sequence (*rat1-ΔNLS*) restored telomere length in *xrn1Δ* cells (Figure 4C). Furthermore, telomeres in *xrn1-E176G* cells expressing the nuclease defective Xrn1 variant were as short as in *xrn1Δ* cells (Figure 4D).

In a deep transcriptome analysis of the genes that are misregulated by the lack of Xrn1, *xrn1Δ* cells showed ∼3-fold reduction of the levels of *TLC1* (58), the RNA component of the telomerase enzyme. However, a 2μ plasmid overexpressing *TLC1* from a galactose inducible promoter did not allow *xrn1Δ* cells to elongate telomeres (Supplementary Figure S2A), although wild-type and *xrn1Δ* cells expressed similar amount of *TLC1* RNA (Supplementary Figure S2B). Thus, telomere shortening in *xrn1Δ* cells cannot be simply explained by the reduction of *TLC1* RNA.

Xrn1 promotes Cdc13 association to telomeres independently of ssDNA generation

Productive association of telomerase to telomeres requires the generation of ssDNA that leads to the recruitment of Cdc13. Cdc13 in turn recruits the telomerase to telomeres by interacting with the telomerase subunit Est1 (14–17). Binding of MRX to telomeres allows Tel1 recruitment that strengthens the association of telomerase to telomeres by phosphorylating unknown targets (23–25). The finding that telomere shortening in *mrxΔ* and *tel1Δ* cells can be suppressed by targeting the telomerase to telomeres through a Cdc13-Est1 protein fusion (70) suggests that MRX/Tel1 promotes Cdc13-Est1 interaction rather than Cdc13 association to telomeres.

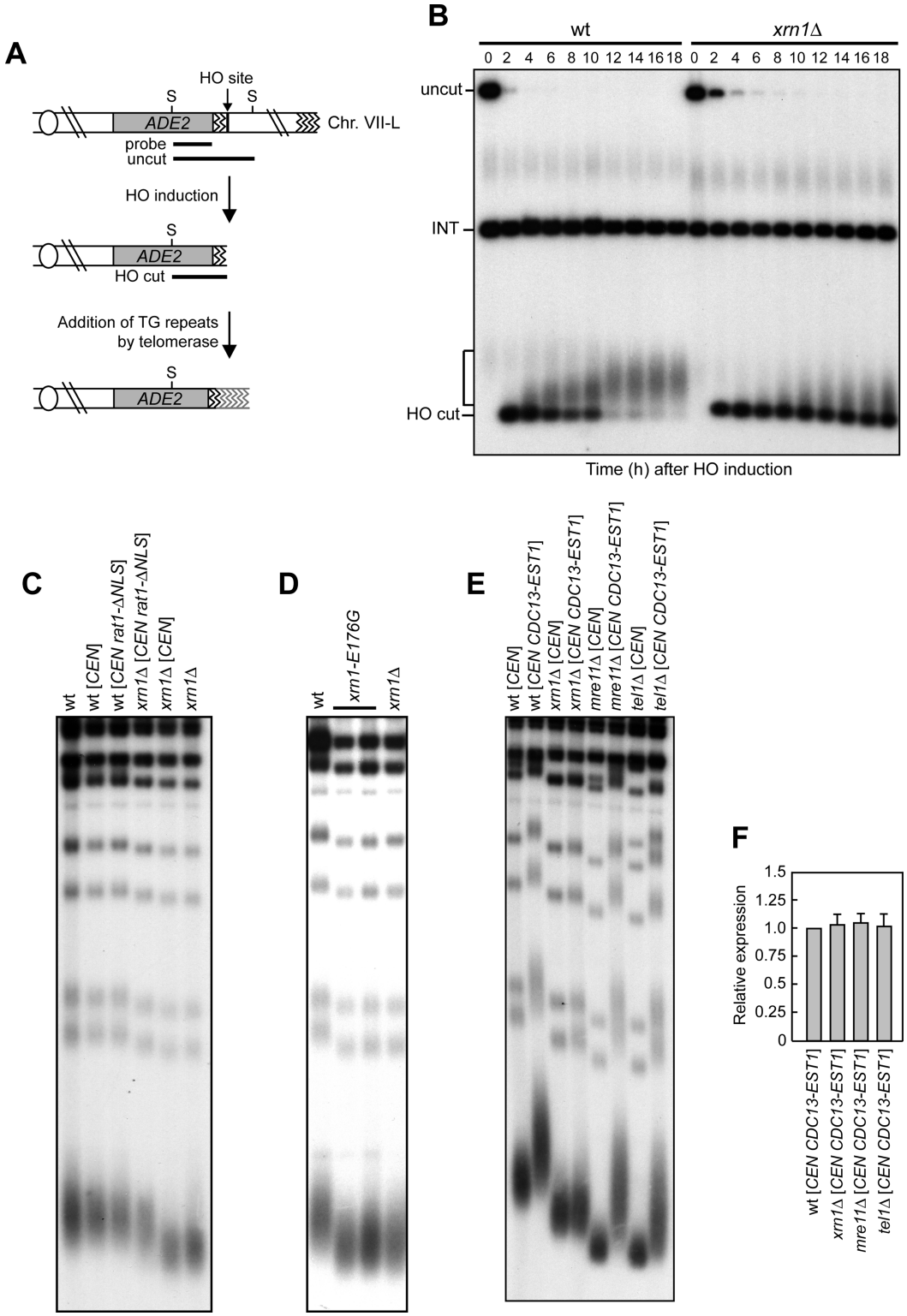

Figure 4. The lack of Xrn1 impairs telomere elongation. (**A**) Schematic representation of the HO-induced short telomere system. The *ADH4* locus on chromosome VII was replaced with a fragment consisting of the *ADE2* gene and 81 bp of TG telomeric sequences (zigzag lines) flanking the recognition site for the HO endonuclease. The centromere is shown as a circle. S, SpeI. (**B**) Elongation of the HO-induced telomere. Cell cultures carrying the system described in A and exponentially growing in raffinose were shifted to galactose at time zero to induce HO expression. SpeI-digested genomic DNA was subjected to Southern blot analysis using an *ADE2* fragment as a probe. A bracket points out new telomere repeats added to the TG telomeric sequences. The band of about 1.6kb (INT) represents the endogenous *ade2-101* gene. (**C**–**E**) XhoI-cut genomic DNA from exponentially growing cells was subjected to Southern blot analysis using a radiolabeled poly(GT) probe. The bar in (D) points out two independent *xrn1-E176G* cell cultures. (**F**) RNA levels of *CDC13-EST1* from cells in (E) were evaluated by quantitative reverse transcriptase PCR (qRT-PCR). Quantities were normalized to *ACT1* RNA levels and compared to that of wild-type cells that was set up to 1. The mean values ±s.d. are represented ($n = 3$).

As Xrn1 was found to promote MRX association at intrachromosomal DSBs (58), we asked whether the expression of a Cdc13-Est1 fusion could restore telomere length in *xrn1Δ* cells. A Cdc13-Est1 fusion expressed from a single-copy plasmid did not suppress the telomere length defect of *xrn1Δ* cells, although it was capable to elongate telomeres in wild type, *mre11Δ* and *tel1Δ* cells (Figure 4E) and all cell cultures expressed similar levels of *CDC13-EST1* mRNA (Figure 4F). This finding suggests that the telomere length defect of *xrn1Δ* cells is not due to MRX dysfunction.

The inability of the Cdc13-Est1 fusion protein to suppress the telomere length defect of *xrn1Δ* cells raises the possibility that Cdc13 itself cannot bind telomeres in the absence of Xrn1. As loss of telomerase is known to be accompanied by recruitment of Cdc13 and Mre11 to telomeres (71), we analyzed the generation of Cdc13 and Mre11 foci before or after loss of telomerase in wild-type and *xrn1Δ* cells. These cells expressed fully functional Cdc13-CFP and Mre11-YFP fusion proteins. As expected, telomerase removal by loss of a plasmid-borne copy of *EST2* resulted in a significant increase of both Mre11-YFP and Cdc13-CFP foci in wild-type cells as early as 25–50 generations after loss of telomerase, with only a subset of them colocalizing (Figure 5A–C). By contrast, *xrn1Δ* cells showed a reduction in the number of Cdc13-CFP foci (Figure 5A and B), but not of Mre11-YFP foci (Figure 5A and C), compared to wild-type, suggesting a requirement for Xrn1 in promoting Cdc13 association to telomeres.

To investigate further this hypothesis, we analyzed the amount of Cdc13 bound at native telomeres in wild-type and *xrn1Δ* cells that were released into a synchronous cell cycle from a G1 arrest (Figure 6A). Cdc13 binding to telomeres peaked in wild type cells 45 min after release, concomitantly with the completion of DNA replication, while it remained very low in *xrn1Δ* cells throughout the time course (Figure 6A and B), although both cell type extracts contained similar amount of Cdc13 (Figure 6C).

Because Cdc13 binds telomeric ssDNA and the lack of Xrn1 impairs ssDNA generation at uncapped telomeres, the reduced Cdc13 association at telomeres in *xrn1Δ* cells might be due to defective generation of telomeric single-stranded overhangs. To investigate this issue, XhoI-cut DNA prepared at different time points after release into the cell cycle from a G1 arrest was subjected to native gel electrophoresis, followed by in-gel hybridization with a C-rich radiolabeled oligonucleotide. As shown in Figure 6D, both wild type and *xrn1Δ* cells showed similar amount of G-tail signals that reached their maximal levels 15–45 min after release, indicating that the lack of Xrn1 does not affect the generation of single-stranded overhangs at capped telomeres.

As generation of telomeric single-stranded overhangs requires the MRX complex (10–12,72), we also analyzed Mre11 association at native telomeres. Wild-type and *xrn1Δ* cells released into a synchronous cell cycle from a G1 arrest showed similar amount of telomere-bound Mre11 (Figure 6E), consistent with the finding that the lack of Xrn1 does not affect the generation of telomeric single-stranded overhangs. Altogether, these data indicate that Xrn1 promotes Cdc13 binding/association to telomeres independently of ssDNA generation.

Xrn1 promotes Cdc13 association at telomeres by downregulating Rif1 level

Deep transcriptome analysis showed that the *RIF1* mRNA level was ∼3-fold higher in *xrn1Δ* cells than in wild-type (58). This mRNA upregulation caused an increase of the Rif1 protein level, as shown by western blot analysis of wild type and *xrn1Δ* protein extracts (Figure 7A), prompting us to test whether this Rif1 upregulation can account for the telomere defects of *xrn1Δ* cells.

As expected from previous findings that Rif1 has a very slight effect on the generation of telomeric ssDNA (73,74), the increased Rif1 levels did not account for the increased temperature resistance of *cdc13-1 xrn1Δ* cells compared to *cdc13-1*. In fact, although *RIF1* deletion decreased the maximum permissive temperature of *cdc13-1* cells (75,76), *cdc13-1 rif1Δ xrn1Δ* cells were more temperature-resistant than *cdc13-1 rif1Δ* cells (Figure 7B), indicating that the suppression of the temperature sensitivity of *cdc13-1* cells by *XRN1* deletion does not require Rif1.

Rif1 was originally identified as a telomere-binding protein that negatively regulates telomerase-mediated telomere elongation (77). Interestingly, the lack of Rif1, although causing a very slight increase of ssDNA formation, yet leads to considerably more Cdc13 binding at telomeres (74). Therefore, Rif1 might block the association/accumulation of Cdc13 at telomeres through a direct mechanism. Consistent with this hypothesis, a 2μ plasmid carrying the *RIF1* gene counteracted the ability of the Cdc13-Est1 fusion to elongate telomeres in wild-type cells (Figure 7C). Thus, we investigated whether the upregulation of Rif1 in *xrn1Δ* cells could explain both the reduced Cdc13 binding and the telomere length defect of the same cells. As shown in Figure 7D, deletion of *RIF1* totally suppressed the telomere length defect of *xrn1Δ* cells. Telomere length in *rif1Δ xrn1Δ* cells was the same as in *rif1Δ* cells (Figure 7D), suggesting that Xrn1 acts in telomere length maintenance by counteracting the effects of Rif1.

As telomeres were much longer in *xrn1Δ rif1Δ* cells than in *xrn1Δ* cells, we could not compare the above cell types for Cdc13 association at native telomeres. Thus, we used the strain with the 81 bp TG repeat sequence adjacent to the HO endonuclease cut site (Figure 4A) (10), where HO induction generates an HO-derived telomere whose length is similar in both *xrn1Δ* and *xrn1Δ rif1Δ* cells. As expected (74), ChIP analysis revealed that the amount of Cdc13 associated to the HO-induced telomere was higher in *rif1Δ* cells than in wild-type (Figure 7E). Furthermore, although all cell type extracts contained similar amounts of Cdc13 (Figure 7F), the lack of Rif1 restored Cdc13 association to telomeres in *xrn1Δ* cells. In fact, the amount of Cdc13 bound at the HO-induced telomere in *xrn1Δ rif1Δ* cells was higher than in *xrn1Δ* cells (Figure 7E). Altogether, these findings indicate that Xrn1 promotes Cdc13 association to telomeres by controlling Rif1 levels.

DISCUSSION

Here we provide evidence that the RNA processing proteins Xrn1 and Rrp6 are involved in telomere metabolism. In particular, we found that the temperature sensitivity of *cdc13-1* mutant cells is partially suppressed by the lack of Rrp6 or

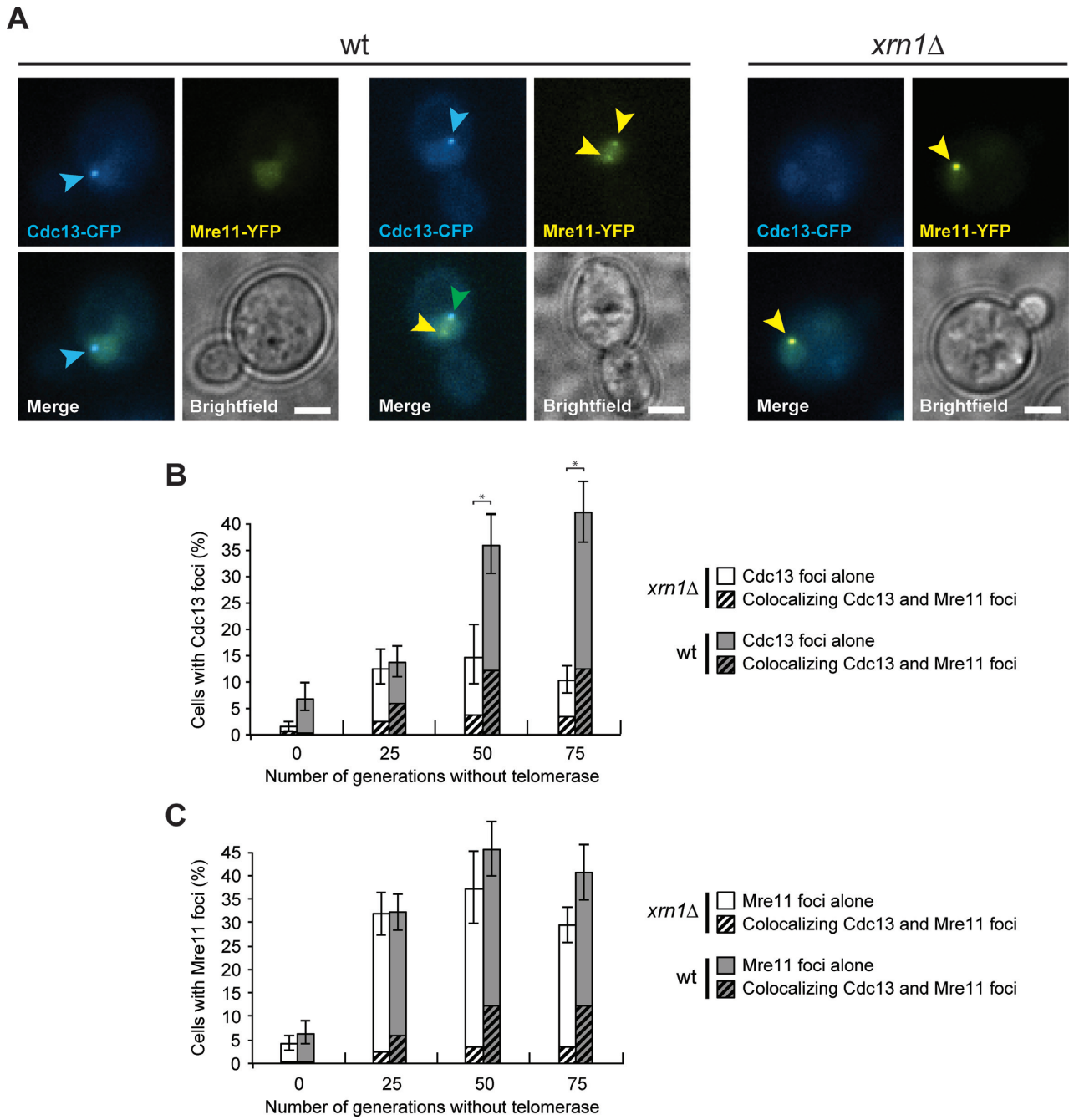

Figure 5. The lack of Xrn1 impairs Cdc13 focus formation. (**A**) Cdc13 and Mre11 localization was examined in *XRN1* (ML968-1D) and *xrn1Δ* (ML968-3B) cells before or 25, 50 and 75 generations after loss of a telomerase-encoding plasmid (pVL291). Yellow arrowheads indicate Mre11-YFP foci, blue arrowheads indicate Cdc13-CFP foci and green arrowhead indicates colocalization between the two proteins. Scale bar: 3 μm. (**B**) *xrn1Δ* cells are impaired for Cdc13 focus formation. Cells in panel A were quantified. Error bars represent 95% confidence intervals ($n = 200$–600). *$P < 0.05$, *t*-test. (**C**) *xrn1Δ* cells are proficient for Mre11 focus formation. Cells in panel A were quantified. Error bars represent 95% confidence intervals ($n = 200$–600).

Xrn1, as well as by Rrp6 or Xrn1 nuclease defective variants, independently of the NMD proteins. The increased temperature resistance of *cdc13-1 xrn1Δ* and *cdc13-1 rrp6Δ* cells is related to their inability to activate the checkpoint.

Checkpoint activation in *cdc13-1* cells is due to the accumulation at telomeres of ssDNA that turns on the checkpoint kinase Mec1. Our data indicate that the defective checkpoint response in *cdc13-1 rrp6Δ* double mutant cells cannot be ascribed to reduced ssDNA generation. Interestingly, Rrp6 was shown to promote the association of RPA (58) and Rad51 (78) at intrachromosomal DSBs in yeast and mammals, respectively, by an unknown mechanism. Thus, one possibility is that Rrp6 modulates directly or indirectly the association to telomeric ssDNA of protein(s) required for checkpoint activation.

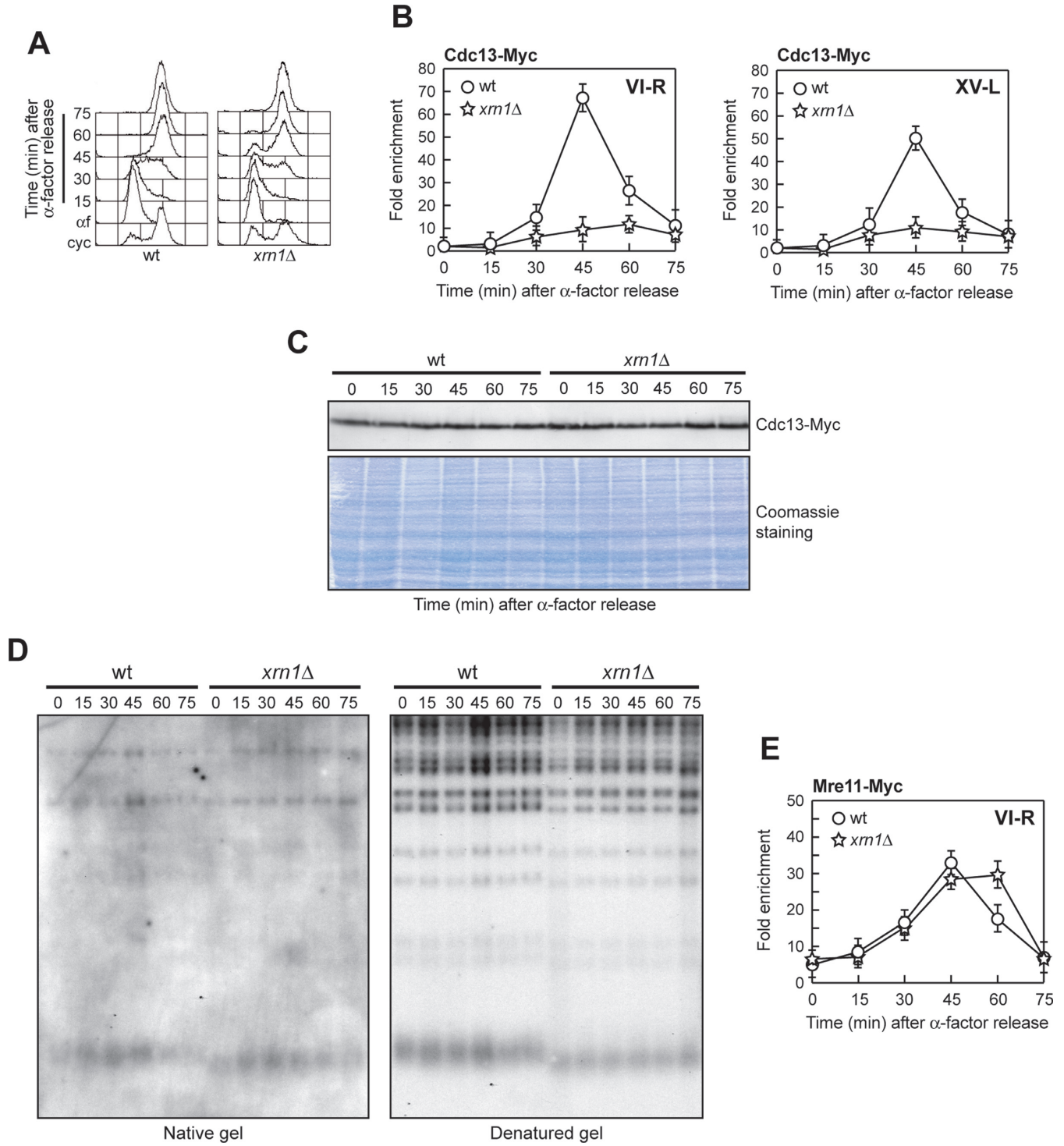

Figure 6. The lack of Xrn1 impairs Cdc13 association but not ssDNA generation at capped telomeres. (**A**–**D**) Exponentially growing cell cultures (cyc) were arrested in G1 with α-factor (αf) and released into the cell cycle. (A) Samples were collected for fluorescence activated cell sorting (FACS). (B) Chromatin samples taken at the indicated times after α-factor release were immunoprecipitated with anti-Myc antibodies. Coimmunoprecipitated DNA was analyzed by quantitative real-time PCR (qPCR) using primer pairs located at telomeres VI-R and XV-L and at the non-telomeric *ARO1* fragment of chromosome IV (CON). Data are expressed as relative fold enrichment of VI-R and XV-L telomere signals over CON signals after normalization to input signals for each primer set. The mean values ±s.d. are represented ($n = 3$). (**C**) Western blot with anti-Myc antibodies of extracts used for the ChIP analysis shown in (B). (D) Genomic DNA prepared from cell samples in (A) was digested with XhoI and the single-strand telomere overhang was visualized by in-gel hybridization (native gel) using an end-labeled C-rich oligonucleotide. The same DNA samples were hybridized with a radiolabeled poly(GT) probe as loading control (denatured gel). (**E**) Chromatin samples taken at the indicated times after α-factor release were immunoprecipitated with anti-Myc antibodies. Coimmunoprecipitated DNA was analyzed by qPCR using primer pairs located at VI-R telomere. Data are expressed as in (B).

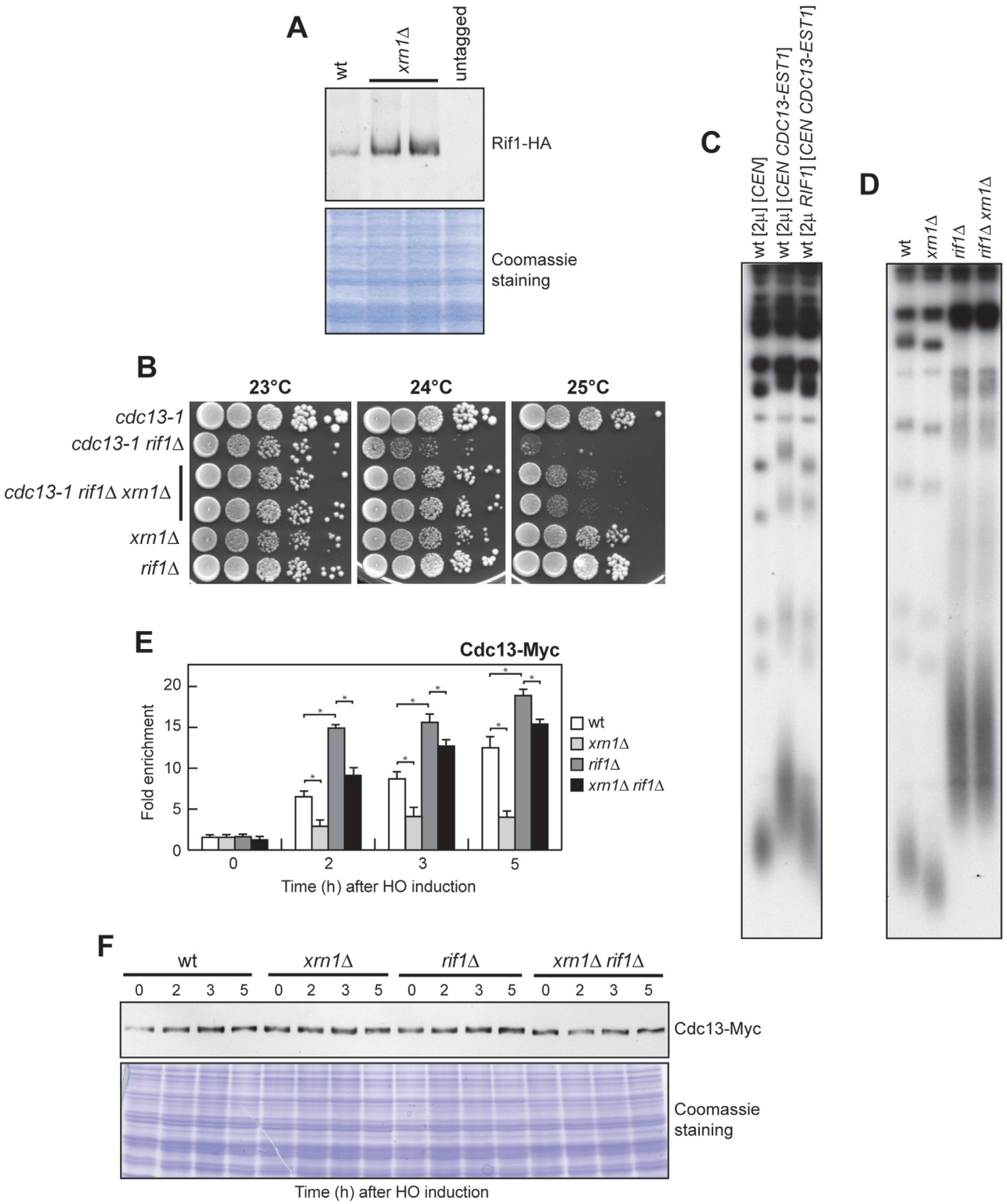

Figure 7. Functional interplays between Xrn1 and Rif1 in telomere length control. (**A**) Protein extracts prepared from exponentially growing cells were subjected to western blot analysis with anti-HA antibodies. (**B**) Cell cultures were grown overnight at 23°C in YEPD and 10-fold serial dilutions were spotted onto YEPD plates. (**C** and **D**) XhoI-cut genomic DNA from exponentially growing cells was subjected to Southern blot analysis using a radiolabeled poly(GT) probe. (**E**) HO expression was induced at time zero by galactose addition to yeast strains carrying the system described in Figure 4A. Chromatin samples taken at the indicated times after HO induction were immunoprecipitated with anti-Myc antibodies and coimmunoprecipitated DNA was analyzed by qPCR using primer pairs located 640 bp centromere-proximal to the HO cutting site and at the non-telomeric *ARO1* fragment of chromosome IV (CON). Data are expressed as relative fold enrichment of TG-HO over CON signal after normalization to input signals for each primer set. The mean values ±s.d. are represented ($n = 3$). *$P < 0.05$, *t*-test. (**F**) Western blot with anti-Myc antibodies of extracts used for the ChIP analysis shown in (E).

By contrast and consistent with the finding that Xrn1 and Rrp6 impairs viability of *cdc13-1* cells by acting in two distinct pathways, the lack of Xrn1 reduces the generation of telomeric ssDNA upon telomere uncapping. This observation, together with the finding that *EXO1* overexpression decreases the maximum permissive temperature of *cdc13-1 xrn1Δ* cells, indicates that Xrn1 participates in checkpoint activation in response to telomere uncapping by promoting the generation of telomeric ssDNA. Interestingly, Xrn1 contributes to generate ssDNA also at intrachromosomal DSBs that are subjected to extensive resection and stimulates Mec1-dependent checkpoint activation, similarly to telomeres following Cdc13 inactivation (29,30,58). By contrast, Xrn1 does not contribute to the generation of single-stranded overhangs at capped telomeres, suggesting a role for Xrn1 in promoting resection specifically at DNA ends that elicit a DNA damage response. Because Xrn1 acts in resection as a cytoplasmic nuclease, one possibility is that the lack of Xrn1 increases the persistence of non-coding RNAs that can inhibit the action of nucleases by annealing with the ssDNA molecules that are generated following telomere uncapping. However, overproduction of the Ribonuclease H1 (Rnh1), which decreases endogenous RNA:DNA hybrids in vivo as well as TERRA levels and R loops at telomeres (79–82), did not restore the temperature sensitivity in *cdc13-1 xrn1Δ* cells (Supplementary Figure S3). A previous deep transcriptome analysis has revealed that the amounts of the majority of mRNAs coding for DNA damage response proteins remained unchanged in *xrn1Δ* cells and the few genes that were misregulated are not obvious candidates (58). Therefore, further work will be required to identify the target(s) by which Xrn1 promotes ssDNA generation and checkpoint activation at uncapped telomeres.

We also show that Xrn1 acts as a cytoplasmic nuclease to maintain telomere length. Strikingly, the lack of Xrn1 dramatically reduces Cdc13 association to telomeres. This defective Cdc13 recruitment is not due to reduced ssDNA generation, as the lack of Xrn1 does not impair ssDNA generation at capped telomeres. On the other hand, the lack of Xrn1 causes upregulation of the *RIF1* mRNA and subsequent increase of the Rif1 protein level. Rif1 was shown to decrease Cdc13 association at telomeres independently of ssDNA generation (74), suggesting that the high Rif1 levels in *xrn1Δ* cells might explain the reduced Cdc13 binding and the telomere length defect of the same cells. Consistent with this hypothesis, we found that the lack of Rif1 completely suppresses the telomere length defect and restores Cdc13 association at telomeres in *xrn1Δ* cells. Altogether, these findings indicate that Xrn1 promotes Cdc13 association to telomeres and telomere elongation independently of ssDNA generation by controlling the amount of Rif1. By contrast, Rif1 is not the Xrn1 target in promoting ssDNA generation and checkpoint activation at uncapped telomeres, as the lack of Xrn1 still suppresses the temperature sensitivity of *cdc13-1 rif1Δ* cells.

In conclusion, Xrn1 appears to have two separate functions at telomeres: (i) it facilitates the generation of ssDNA and checkpoint activation at uncapped telomeres; (ii) it maintains telomere length independently of ssDNA generation by downregulating the amount of Rif1, which in turn counteracts Cdc13 association to telomeres. As RNA-processing factors are evolutionarily conserved and telomere protection is critical for preserving genetic stability and counteracting cancer development, our findings highlight novel mechanisms through which RNA processing proteins can preserve genome integrity.

SUPPLEMENTARY DATA

Supplementary Data are available at NAR Online.

ACKNOWLEDGEMENTS

We are grateful to A. Aguilera, J.S. Butler, D. Gottschling, A.W. Johnson, V. Lundblad and R. Wellinger for strains and plasmids. We thank G. Lucchini for critical reading of the manuscript.

FUNDING

Associazione Italiana per la Ricerca sul Cancro (AIRC) [IG grant 15210]; Progetti di Ricerca di Interesse Nazionale (PRIN) 2015 [to M.P.L.]; Danish Council for Independent Research and the Villum Foundation (to M.L.); Fellowship from Fondazione Italiana per la Ricerca sul Cancro (FIRC) (to C.C.). Funding for open access charge: AIRC [IG grant 15210 to M.P.L].
Conflict of interest statement. None declared.

REFERENCES

1. Wellinger,R.J. and Zakian,V.A. (2012) Everything you ever wanted to know about *Saccharomyces cerevisiae* telomeres: beginning to end. *Genetics*, **191**, 1073–1105.
2. Bonetti,D., Martina,M., Falcettoni,M. and Longhese,M.P. (2014) Telomere-end processing: mechanisms and regulation. *Chromosoma*, **123**, 57–66.
3. Henderson,E.R. and Blackburn,E.H. (1989) An overhanging 3′ terminus is a conserved feature of telomeres. *Mol. Cell. Biol.*, **9**, 345–348.
4. Wellinger,R.J., Wolf,A.J. and Zakian,V.A. (1993) *Saccharomyces* telomeres acquire single-strand $TG_{1\text{-}3}$ tails late in S phase. *Cell*, **72**, 51–60.
5. Pfeiffer,V. and Lingner,J. (2013) Replication of telomeres and the regulation of telomerase. *Cold Spring Harb. Perspect. Biol.*, **5**, a010405.
6. Dionne,I. and Wellinger,R.J. (1996) Cell cycle-regulated generation of single-stranded G-rich DNA in the absence of telomerase. *Proc. Natl. Acad. Sci. U.S.A.*, **93**, 13902–13907.
7. Wellinger,R.J., Ethier,K., Labrecque,P. and Zakian,V.A. (1996) Evidence for a new step in telomere maintenance. *Cell*, **85**, 423–433.
8. Soudet,J., Jolivet,P. and Teixeira,M.T. (2014) Elucidation of the DNA end-replication problem in *Saccharomyces cerevisiae*. *Mol. Cell*, **53**, 954–964.
9. Faure,V., Coulon,S., Hardy,J. and Géli,V. (2010) Cdc13 and telomerase bind through different mechanisms at the lagging- and leading-strand telomeres. *Mol. Cell*, **38**, 842–852.
10. Diede,S.J. and Gottschling,D.E. (2001) Exonuclease activity is required for sequence addition and Cdc13p loading at a de novo telomere. *Curr. Biol.*, **11**, 1336–1340.
11. Larrivée,M., LeBel,C. and Wellinger,R.J. (2004) The generation of proper constitutive G-tails on yeast telomeres is dependent on the MRX complex. *Genes Dev.*, **18**, 1391–1396.
12. Bonetti,D., Martina,M., Clerici,M., Lucchini,G. and Longhese,M.P. (2009) Multiple pathways regulate 3′ overhang generation at *S. cerevisiae* telomeres. *Mol. Cell*, **35**, 70–81.
13. Gao,H., Cervantes,R.B., Mandell,E.K., Otero,J.H. and Lundblad,V. (2007) RPA-like proteins mediate yeast telomere function. *Nat. Struct. Mol. Biol.*, **14**, 208–214.

14. Nugent,C.I., Hughes,T.R., Lue,N.F. and Lundblad,V. (1996) Cdc13p: a single-strand telomeric DNA-binding protein with a dual role in yeast telomere maintenance. *Science*, **274**, 249–252.
15. Evans,S.K. and Lundblad,V. (1999) Est1 and Cdc13 as comediators of telomerase access. *Science*, **286**, 117–120.
16. Pennock,E., Buckley,K. and Lundblad,V. (2001) Cdc13 delivers separate complexes to the telomere for end protection and replication. *Cell*, **104**, 387–396.
17. Bianchi,A., Negrini,S. and Shore,D. (2004) Delivery of yeast telomerase to a DNA break depends on the recruitment functions of Cdc13 and Est1. *Mol. Cell*, **16**, 139–146.
18. Nakada,D., Matsumoto,K. and Sugimoto,K. (2003) ATM-related Tel1 associates with double-strand breaks through an Xrs2-dependent mechanism. *Genes Dev.*, **17**, 1957–1962.
19. Chang,M., Arneric,M. and Lingner,J. (2007) Telomerase repeat addition processivity is increased at critically short telomeres in a Tel1-dependent manner in *Saccharomyces cerevisiae*. *Genes Dev.*, **21**, 2485–2494.
20. Hector,R.E., Shtofman,R.L., Ray,A., Chen,B.R., Nyun,T., Berkner,K.L. and Runge,K.W. (2007) Tel1p preferentially associates with short telomeres to stimulate their elongation. *Mol. Cell*, **27**, 851–858.
21. Sabourin,M., Tuzon,C.T. and Zakian,V.A. (2007) Telomerase and Tel1p preferentially associate with short telomeres in *S. cerevisiae*. *Mol. Cell*, **27**, 550–561.
22. McGee,J.S., Phillips,J.A., Chan,A., Sabourin,M., Paeschke,K. and Zakian,V.A. (2010) Reduced Rif2 and lack of Mec1 target short telomeres for elongation rather than double-strand break repair. *Nat. Struct. Mol. Biol.*, **17**, 1438–1445.
23. Tseng,S.F., Lin,J.J. and Teng,S.C. (2006) The telomerase-recruitment domain of the telomere binding protein Cdc13 is regulated by Mec1p/Tel1p-dependent phosphorylation. *Nucleic Acids Res.*, **34**, 6327–6336.
24. Gao,H., Toro,T.B., Paschini,M., Braunstein-Ballew,B., Cervantes,R.B. and Lundblad,V. (2010) Telomerase recruitment in *Saccharomyces cerevisiae* is not dependent on Tel1-mediated phosphorylation of Cdc13. *Genetics*, **186**, 1147–1159.
25. Wu,Y., DiMaggio,P.A. Jr, Perlman,D.H., Zakian,V.A. and Garcia,B.A. (2013) Novel phosphorylation sites in the *S. cerevisiae* Cdc13 protein reveal new targets for telomere length regulation. *J. Proteome Res.*, **12**, 316–327.
26. Goudsouzian,L.K., Tuzon,C.T. and Zakian,V.A. (2006) *S.cerevisiae* Tel1p and Mre11p are required for normal levels of Est1p and Est2p telomere association. *Mol. Cell*, **24**, 603–610.
27. Qi,H. and Zakian,V.A. (2000) The *Saccharomyces* telomere-binding protein Cdc13p interacts with both the catalytic subunit of DNA polymerase alpha and the telomerase-associated est1 protein. *Genes Dev.*, **14**, 1777–1788.
28. Grossi,S., Puglisi,A., Dmitriev,P.V., Lopes,M. and Shore,D. (2004) Pol12, the B subunit of DNA polymerase alpha, functions in both telomere capping and length regulation. *Genes Dev.*, **18**, 992–1006.
29. Garvik,B., Carson,M. and Hartwell,L. (1995) Single-stranded DNA arising at telomeres in *cdc13* mutants may constitute a specific signal for the *RAD9* checkpoint. *Mol. Cell. Biol.*, **15**, 6128–6138.
30. Lydall,D. and Weinert,T. (1995) Yeast checkpoint genes in DNA damage processing: implications for repair and arrest. *Science*, **270**, 1488–1491.
31. Vodenicharov,M.D. and Wellinger,R.J. (2006) DNA degradation at unprotected telomeres in yeast is regulated by the CDK1 (Cdc28/Clb) cell-cycle kinase. *Mol. Cell*, **24**, 127–137.
32. Grandin,N., Reed,S.I. and Charbonneau,M. (1997) Stn1, a new *Saccharomyces cerevisiae* protein, is implicated in telomere size regulation in association with Cdc13. *Genes Dev.*, **11**, 512–527.
33. Grandin,N., Damon,C. and Charbonneau,M. (2001) Ten1 functions in telomere end protection and length regulation in association with Stn1 and Cdc13. *EMBO J.*, **20**, 1173–1183.
34. Puglisi,A., Bianchi,A., Lemmens,L., Damay,P. and Shore,D. (2008) Distinct roles for yeast Stn1 in telomere capping and telomerase inhibition. *EMBO J.*, **27**, 2328–2339.
35. Xu,L., Petreaca,R.C., Gasparyan,H.J., Vu,S. and Nugent,C.I. (2009) *TEN1* is essential for *CDC13*-mediated telomere capping. *Genetics*, **183**, 793–810.
36. Maringele,L. and Lydall,D. (2002) *EXO1*-dependent single-stranded DNA at telomeres activates subsets of DNA damage and spindle checkpoint pathways in budding yeast *yku70Δ* mutants. *Genes Dev.*, **16**, 1919–1933.
37. Zubko,M.K., Guillard,S. and Lydall,D. (2004) Exo1 and Rad24 differentially regulate generation of ssDNA at telomeres of *Saccharomyces cerevisiae cdc13-1* mutants. *Genetics*, **168**, 103–115.
38. Parker,R. (2012) RNA degradation in *Saccharomyces cerevisae*. *Genetics*, **191**, 671–702.
39. Nagarajan,V.K., Jones,C.I., Newbury,S.F. and Green,P.J. (2013) XRN 5′-3′ exoribonucleases: structure, mechanisms and functions. *Biochim. Biophys. Acta*, **1829**, 590–603.
40. Houseley,J., LaCava,J. and Tollervey,D. (2006) RNA-quality control by the exosome. *Nat. Rev. Mol. Cell Biol.*, **7**, 529–539.
41. Askree,S.H., Yehuda,T., Smolikov,S., Gurevich,R., Hawk,J., Coker,C., Krauskopf,A., Kupiec,M. and McEachern,M.J. (2004) A genome-wide screen for *Saccharomyces cerevisiae* deletion mutants that affect telomere length. *Proc. Natl. Acad. Sci. U.S.A.*, **101**, 8658–8663.
42. Ungar,L., Yosef,N., Sela,Y., Sharan,R., Ruppin,E. and Kupiec,M. (2009) A genome-wide screen for essential yeast genes that affect telomere length maintenance. *Nucleic Acids Res.*, **37**, 3840–3849.
43. Azzalin,C.M., Reichenbach,P., Khoriauli,L., Giulotto,E. and Lingner,J. (2007) Telomeric repeat containing RNA and RNA surveillance factors at mammalian chromosome ends. *Science*, **318**, 798–801.
44. Chawla,R., Redon,S., Raftopoulou,C., Wischnewski,H., Gagos,S. and Azzalin,C.M. (2011) Human UPF1 interacts with TPP1 and telomerase and sustains telomere leading-strand replication. *EMBO J.*, **30**, 4047–4058.
45. Lew,J.E., Enomoto,S. and Berman,J. (1998) Telomere length regulation and telomeric chromatin require the nonsense-mediated mRNA decay pathway. *Mol. Cell. Biol.*, **18**, 6121–6130.
46. Dahlseid,J.N., Lew-Smith,J., Lelivelt,M.J., Enomoto,S., Ford,A., Desruisseaux,M., McClellan,M., Lue,N., Culbertson,M.R. and Berman,J. (2003) mRNAs encoding telomerase components and regulators are controlled by *UPF* genes in *Saccharomyces cerevisiae*. *Eukaryot. Cell*, **2**, 134–142.
47. Addinall,S.G., Holstein,E.M., Lawles,C., Yu,M., Chapman,K., Banks,A.P., Ngo,H.P., Maringele,L., Taschuk,M., Young,A. *et al.* (2011) Quantitative fitness analysis shows that NMD proteins and many other protein complexes suppress or enhance distinct telomere cap defects. *PLoS Genet.*, **7**, e1001362.
48. Holstein,E.M., Clark,K.R. and Lydall,D. (2014) Interplay between nonsense-mediated mRNA decay and DNA damage response pathways reveals that Stn1 and Ten1 are the key CST telomere-cap components. *Cell Rep.*, **7**, 1259–1269.
49. Shukla,S., Schmidt,J.C., Goldfarb,K.C., Cech,T.R. and Parker,R. (2016) Inhibition of telomerase RNA decay rescues telomerase deficiency caused by dyskerin or PARN defects. *Nat. Struct. Mol. Biol.*, **23**, 286–292.
50. Luke,B., Panza,A., Redon,S., Iglesias,N., Li,Z. and Lingner,J. (2008) The Rat1p 5′ to 3′ exonuclease degrades telomeric repeat-containing RNA and promotes telomere elongation in *Saccharomyces cerevisiae*. *Mol. Cell*, **32**, 465–477.
51. Pfeiffer,V. and Lingner,J. (2012) TERRA promotes telomere shortening through exonuclease 1-mediated resection of chromosome ends. *PLoS Genet.*, **8**, e1002747.
52. Iglesias,N., Redon,S., Pfeiffer,V., Dees,M., Lingner,J. and Luke,B. (2011) Subtelomeric repetitive elements determine TERRA regulation by Rap1/Rif and Rap1/Sir complexes in yeast. *EMBO Rep.*, **12**, 587–593.
53. Bonetti,D., Clerici,M., Manfrini,N., Lucchini,G. and Longhese,M.P. (2010) The MRX complex plays multiple functions in resection of Yku- and Rif2-protected DNA ends. *PLoS One*, **5**, e14142.
54. Viscardi,V., Bonetti,D., Cartagena-Lirola,H., Lucchini,G. and Longhese,M.P. (2007) MRX-dependent DNA damage response to short telomeres. *Mol. Biol. Cell*, **18**, 3047–3058.
55. Eckert-Boulet,N., Rothstein,R. and Lisby,M. (2011) Cell biology of homologous recombination in yeast. *Methods Mol. Biol.*, **745**, 523–536.
56. Heim,R. and Tsien,R.Y. (1996) Engineering green fluorescent protein for improved brightness, longer wavelengths and fluorescence resonance energy transfer. *Curr. Biol.*, **6**, 178–182.

57. Ormo,M., Cubitt,A.B., Kallio,K., Gross,L.A., Tsien,R.Y. and Remington,S.J. (1996) Crystal structure of the Aequorea victoria green fluorescent protein. *Science*, **273**, 1392–1395.
58. Manfrini,N., Trovesi,C., Wery,M., Martina,M., Cesena,D., Descrimes,M., Morillon,A., d'Adda di Fagagna,F. and Longhese,M.P. (2015) RNA-processing proteins regulate Mec1/ATR activation by promoting generation of RPA-coated ssDNA. *EMBO Rep.*, **16**, 221–231.
59. Page,A.M., Davis,K., Molineux,C., Kolodner,R.D. and Johnson,A.W. (1998) Mutational analysis of exoribonuclease I from *Saccharomyces cerevisiae*. *Nucleic Acids Res.*, **26**, 3707–3716.
60. Burkard,K.T. and Butler,J.S. (2000) A nuclear 3′-5′ exonuclease involved in mRNA degradation interacts with Poly(A) polymerase and the hnRNA protein Npl3p. *Mol. Cell. Biol.*, **20**, 604–616.
61. Johnson,A.W. (1997) Rat1p and Xrn1p are functionally interchangeable exoribonucleases that are restricted to and required in the nucleus and cytoplasm, respectively. *Mol. Cell. Biol.*, **17**, 6122–6130.
62. Isken,O. and Maquat,L.E. (2008) The multiple lives of NMD factors: balancing roles in gene and genome regulation. *Nat. Rev. Genet.*, **9**, 699–712.
63. Enomoto,S., Glowczewski,L., Lew-Smith,J. and Berman,J.G. (2004) Telomere cap components influence the rate of senescence in telomerase-deficient yeast cells. *Mol. Cell. Biol.*, **24**, 837–845.
64. Chandra,A., Hughes,T.R., Nugent,C.I. and Lundblad,V. (2001) Cdc13 both positively and negatively regulates telomere replication. *Genes Dev.*, **15**, 404–414.
65. Grandin,N., Damon,C. and Charbonneau,M. (2000) Cdc13 cooperates with the yeast Ku proteins and Stn1 to regulate telomerase recruitment. *Mol. Cell. Biol.*, **20**, 8397–8408.
66. He,F., Li,X., Spatrick,P., Casillo,R., Dong,S. and Jacobson,A. (2003) Genome-wide analysis of mRNAs regulated by the nonsense-mediated and 5′ to 3′ mRNA decay pathways in yeast. *Mol. Cell*, **12**, 1439–1452.
67. Petreaca,R.C., Chiu,H.C. and Nugent,C.I. (2007) The role of Stn1p in *Saccharomyces cerevisiae* telomere capping can be separated from its interaction with Cdc13p. *Genetics*, **177**, 1459–1474.
68. Mantiero,D., Clerici,M., Lucchini,G. and Longhese,M.P. (2007) Dual role for *Saccharomyces cerevisiae* Tel1 in the checkpoint response to double-strand breaks. *EMBO Rep.*, **8**, 380–387.
69. Diede,S.J. and Gottschling,D.E. (1999) Telomerase-mediated telomere addition in vivo requires DNA primase and DNA polymerases alpha and delta. *Cell*, **99**, 723–733.
70. Tsukamoto,Y., Taggart,A.K. and Zakian,V.A. (2001) The role of the Mre11-Rad50-Xrs2 complex in telomerase- mediated lengthening of *Saccharomyces cerevisiae* telomeres. *Curr. Biol.*, **11**, 1328–1335.
71. Khadaroo,B., Teixeira,M.T., Luciano,P., Eckert-Boulet,N., Germann,S.M., Simon,M.N., Gallina,I., Abdallah,P., Gilson,E., Géli,V. and Lisby,M. (2009) The DNA damage response at eroded telomeres and tethering to the nuclear pore complex. *Nat. Cell Biol.*, **11**, 980–987.
72. Chai,W., Sfeir,A.J., Hoshiyama,H., Shay,J.W. and Wright,W.E. (2006) The involvement of the Mre11/Rad50/Nbs1 complex in the generation of G-overhangs at human telomeres. *EMBO Rep.*, **7**, 225–230.
73. Bonetti,D., Clerici,M., Anbalagan,S., Martina,M., Lucchini,G. and Longhese,M.P. (2010) Shelterin-like proteins and Yku inhibit nucleolytic processing of *Saccharomyces cerevisiae* telomeres. *PLoS Genet.*, **6**, e1000966.
74. Ribeyre,C. and Shore,D. (2012) Anticheckpoint pathways at telomeres in yeast. *Nat. Struct. Mol. Biol.*, **19**, 307–313.
75. Anbalagan,S., Bonetti,D., Lucchini,G. and Longhese,M.P. (2011) Rif1 supports the function of the CST complex in yeast telomere capping. *PLoS Genet.*, **7**, e1002024.
76. Xue,Y., Rushton,M.D. and Maringele,L. (2011) A novel checkpoint and RPA inhibitory pathway regulated by Rif1. *PLoS Genet.*, **7**, e1002417.
77. Hardy,C.F., Sussel,L. and Shore,D. (1992) A RAP1-interacting protein involved in transcriptional silencing and telomere length regulation. *Genes Dev.*, **6**, 801–814.
78. Marin-Vicente,C., Domingo-Prim,J., Eberle,A.B. and Visa,N. (2015) RRP6/EXOSC10 is required for the repair of DNA double-strand breaks by homologous recombination. *J. Cell Sci.*, **128**, 1097–1107.
79. Balk,B., Maicher,A., Dees,M., Klermund,J., Luke-Glaser,S., Bender,K. and Luke,B. (2013) Telomeric RNA-DNA hybrids affect telomere-length dynamics and senescence. *Nat. Struct. Mol. Biol.*, **20**, 1199–1205.
80. Gavaldá,S., Gallardo,M., Luna,R. and Aguilera,A. (2013) R-loop mediated transcription-associated recombination in *trf4Δ* mutants reveals new links between RNA surveillance and genome integrity. *PLoS One*, **8**, e65541.
81. Arora,R., Lee,Y., Wischnewski,H., Brun,C.M., Schwarz,T. and Azzalin,C.M. (2014) RNaseH1 regulates TERRA-telomeric DNA hybrids and telomere maintenance in ALT tumour cells. *Nat. Commun.*, **5**, 5220–5230.
82. Yu,T.Y., Kao,Y.W. and Lin,J.J. (2014) Telomeric transcripts stimulate telomere recombination to suppress senescence in cells lacking telomerase. *Proc. Natl. Acad. Sci. U.S.A.*, **111**, 3377–3382.